



NUMERICAL ANALYSIS OF NATURAL CONVECTION HEAT TRANSFER FROM PARTIALLY OPEN CAVITIES HEATED AT ONE WALL

Ayla DOĞAN*, S. BAYSAL** and Senol BASKAYA**

*Department of Mechanical Engineering, Akdeniz University,
07058 Campus, Antalya, Turkey, ayladogan@akdeniz.edu.tr

**Department of Mechanical Engineering, Gazi University,
06570 Maltepe, Ankara, Turkey, baskaya@gazi.edu.tr

(Geliş Tarihi: 12. 11. 2008, Kabul Tarihi: 29. 01. 2009)

Abstract: In this study, the heat transfer by natural convection from partially open cavities with one wall heated was investigated numerically. The aim of this study was the steady state investigation of the natural convection heat transfer inside the cavity under uniform heat fluxes (q''), different opening ratios (OR), tilt angles (θ) and cavity aspect ratios (AR) for top and center opening positions. For this purpose, the equations of conservation of mass, momentum and energy were solved using adequate boundary conditions by means of the PHOENICS code. According to the results obtained, the average heat transfer coefficient increases and the average wall temperature decreases, with the increase in opening ratio and decrease in the tilt angle. Best heat transfer was obtained with the maximum aspect ratio for opening ratio of 0.75 and tilt angle of -10° .

Keywords: Natural convection, Opening ratio, Aspect ratio, CFD.

BİR DUVARI ISITILMIŞ KISMİ AÇIK HACİMLERDEN DOĞAL KONVEKSİYONLA ISI TRANSFERİNİN SAYISAL ANALİZİ

Özet: Bu çalışmada, bir duvarı ısıtılmış kısmi açık hacimlerden doğal konveksiyonla ısı transferi sayısal olarak incelenmiştir. Çalışmanın amacı, uniform ısı akısı (q'') altındaki boşluk içerisinde, sürekli şartlarda, farklı açıklık oranları (AO), eğim açıları (EA) ve geometrik oranlarda (GO), üstten ve merkezden açık konumlar için doğal konveksiyonla ısı transferinin incelenmesidir. Bu amaçla, kütle, momentum ve enerji korunum denklemleri uygun sınır şartları kullanılarak PHOENICS kodu ile çözülmüştür. Elde edilen sonuçlara göre, açıklık oranının artması ve eğim açısının azalmasıyla, ortalama ısı transfer katsayısı artmakta ve ortalama duvar sıcaklığı azalmaktadır. Geometrik oranın maksimum, açıklık oranının 0.75 ve eğim açısının -10° olduğu durumda en iyi ısı transferi elde edilmiştir.

Anahtar kelimeler: Doğal konveksiyon, Açıklık oranı, Geometrik oran, HAD.

NOMENCLATURE

a	opening height [m]	θ	tilt angle [degree]
AR	aspect ratio [=H/W]	u	velocity component in x-direction [m/s]
c_p	specific heat [J/kg K]	v	velocity component in y-direction [m/s]
g	gravitational acceleration [m/s^2]	W	length of the cavity, [m]
Gr_H	Grashof number [= $g\beta q'' H^4 / kv^2$]	x, y	Cartesian coordinates
h_{avg}	average heat transfer coefficient [$W/m^2 K$]		
H	height of the cavity [m]		
k	thermal conductivity [W/m K]		
Nu	average Nusselt number [= $h_{avg} H/k$]		
OR	opening ratio [a/H]		
p	pressure [N/m^2]		
Pr	Prandtl number		
Ra_H	Rayleigh number [= $Gr_H Pr$]		
T	temperature [$^\circ C$]		
q''	heat flux [W/m^2]		
			Greek symbols
		α	thermal diffusivity [m^2/s]
		β	thermal expansion coefficient [1/K]
		μ	dynamic viscosity [kg/ms]
		ν	kinematic viscosity [m^2/s]
		ρ	density [kg/m ³]
			Subscripts
		∞	ambient value
		w	wall

INTRODUCTION

Partially open cavities are common in a wide range of engineering applications such as open cavity solar thermal receivers, uncovered flat plate solar collectors having rows of vertical strip, electronic chips, room heating, etc. The researchers of cavity heating therefore have had increased interest in the analysis of fluid flow and heat transfer in these situations.

There are numerous studies in the literature regarding natural convection problems in rectangular and square cavities subjected to heat flux and temperature. Costa (2002), investigated laminar natural convection in differentially heated rectangular enclosures with vertical diffusive walls. The proposed procedure was examined, by comparing the obtained results with those achieved from the complete two dimensional numerical simulation of the conjugate heat transfer problem, occurring in the complete enclosure, with diffusive walls. Aydin et al. (1999), investigated numerically natural convection in rectangular enclosures heated from one side and cooled from the ceiling. They analyzed the steady natural convection of air in a two dimensional enclosure using a stream function-vorticity formulation. Experiments and numerical computations were performed for turbulent natural convection in a large air-filled cavity by Salat et al. (2004). They made numerical simulations for both adiabatic conditions, and experimentally measured temperature on the horizontal walls. Another study was conducted by Di Piazza and Ciofalo (2000), who made direct numerical two-dimensional simulations for the free convective flow of low-Prandtl number (0.0321), for a slender cavity of $AR=4$. Arcidiacono et al. (2001) studied a square cavity ($AR=1$), which had isothermal side walls and adiabatic top and bottom walls. Chang and Tsay (2001) examined the laminar natural convection in an enclosure induced by a heated backward step. The effects of Rayleigh number, Prandtl number, and geometrical size of the enclosure on the flow structure and heat transfer characteristics were investigated in detail. Leong and Tan (2001) conducted an experimental investigation into freezing of n-paraffin solution in a rectangular enclosure having a vertical isothermal side wall and other adiabatic walls. Nithyadevi et al. (2007) numerically investigated the effect of aspect ratio on the natural convection of a fluid contained in a rectangular cavity with partially thermally active side walls. The active part of the left side wall was selected at a higher temperature than that of the right side wall. The top and bottom of the cavity and inactive part of the side walls were thermally insulated. Another study was conducted experimentally and numerically by Poujol (2000), who investigated transient natural convection in a square cavity heated with a time-dependent heat flux on one vertical wall, and cooled by maintaining the opposite wall, at a constant temperature. Basak et al. (2006) conducted a study on the effect of thermal boundary conditions on natural convection flows within a square

cavity. They investigated the steady laminar natural convection flow in a square cavity with uniformly and non-uniformly heated bottom wall, and adiabatic top wall maintaining a constant temperature at the cold vertical wall. The numerical procedure adopted in this study was used over a wide range of parameters (Rayleigh number Ra , $10^3 \leq Ra \leq 10^5$ and Prandtl number Pr , $0.7 \leq Pr \leq 10$) with respect to continuous and discontinuous Dirichlet boundary conditions. Elsayed and Chakroun (1999) studied the effect of aperture geometry on heat transfer in tilted partially open cavities. They carried out experiments to study the effect of the aperture geometry on the heat transfer between the cavity and surrounding air. They examined different geometrical arrangements, different opening ratios, and tilt angles. Polat and Bilgen (2002) numerically investigated laminar natural convection in inclined open shallow cavities for Rayleigh numbers from 10^3 to 10^7 , cavity aspect ratio from 1 to 0.125. Bilgen and Oztop (2005) studied numerically natural convection heat transfer in partially open inclined square cavities. They investigated numerically the steady-state heat transfer by laminar natural convection in a two dimensional partially open cavity. Kasayapanand (2007) investigated the numerical modeling of the electric field effect on natural convection in the partially open square cavities, by using a computational fluid dynamics technique.

In the present study, the steady state investigation of laminar natural convection heat transfer inside a partially open cavity under uniform heat fluxes (q''), different opening ratios (OR), tilt angles (θ) and cavity aspect ratios (AR), for top and center opening positions was performed. To the authors knowledge these parameters have not been investigated yet, numerically.

NUMERICAL MODEL

The geometry of the partially open cavity and coordinate system of the problem under consideration is depicted in Fig. 1.

One side of the cavity is subjected to- uniform heat flux and all other sides of the cavity are assumed to be perfectly insulated. The heat transfer between the cavity and the surroundings is affected by the geometrical parameters: the aspect ratio ($AR= H/W$), opening ratio ($OR= a/H$) and tilt angle ($\theta=$ degree).

Two dimensional computational cell structures and its distribution are shown Fig. 2. The numerical code employed for the present study was rigorously verified.

First the present study was carried out to ensure that solution is grid independent. Accordingly, 90×90 cell numbers and 5000 sweeps are determined to be suitable for this study.

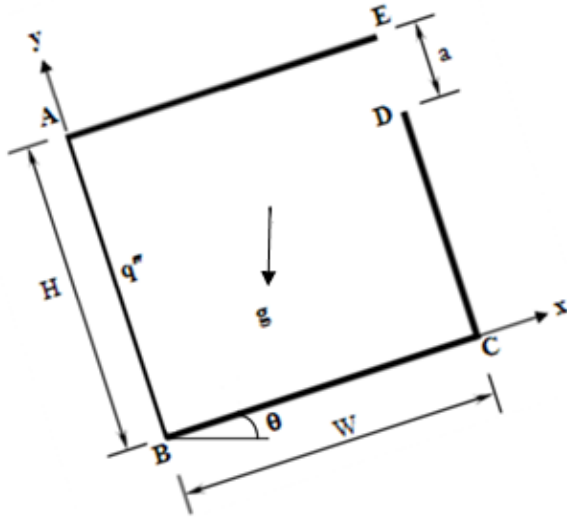


Figure 1. Geometry of partially open cavity.

In order to check the adequacy of the present study, the obtained results are compared with experimental measurements by Elsayed and Chakroun (Elsayed and Chakroun, 1999). As can be seen in Fig. 3, there is a good agreement between numerical and experimental results. The maximum difference between experimental and CFD values does not exceed 12 % for angles of -15° , 0° and 15° . This can be considered as a sufficient verification of the computational domain and numerical procedures applied in the present study.

MATHEMATICAL FORMULATION

The continuity, momentum and energy equations for a two dimensional incompressible laminar flow have been

solved using appropriate boundary conditions by means of the PHOENICS CFD code. Following assumptions have been made: there is no viscous dissipation, the gravity acts in the vertical direction, the fluid properties are constant, the fluid density changes with temperature only, and radiation heat exchange was assumed negligible. At steady-state conditions using above assumptions, the governing equations for the two dimensional laminar flow can be expressed as given below:

Continuity equation:

$$\frac{\partial(\rho u)}{\partial x} + \frac{\partial(\rho v)}{\partial y} = 0 \quad (1)$$

x- momentum equation:

$$\frac{\partial(\rho u^2)}{\partial x} + \frac{\partial(\rho uv)}{\partial y} = -\frac{\partial P}{\partial x} + \mu \left(\frac{\partial^2 u}{\partial x^2} + \frac{\partial^2 u}{\partial y^2} \right) + g \sin \theta (\rho_\infty - \rho) \quad (2)$$

y- momentum equation:

$$\frac{\partial(\rho uv)}{\partial x} + \frac{\partial(\rho v^2)}{\partial y} = -\frac{\partial P}{\partial y} + \mu \left(\frac{\partial^2 v}{\partial x^2} + \frac{\partial^2 v}{\partial y^2} \right) + g \cos \theta (\rho_\infty - \rho) \quad (3)$$

Energy equation:

$$u \frac{\partial T}{\partial x} + v \frac{\partial T}{\partial y} = \alpha \left(\frac{\partial^2 T}{\partial x^2} + \frac{\partial^2 T}{\partial y^2} \right) \quad (4)$$

The reference density, ρ_∞ , has been calculated from the

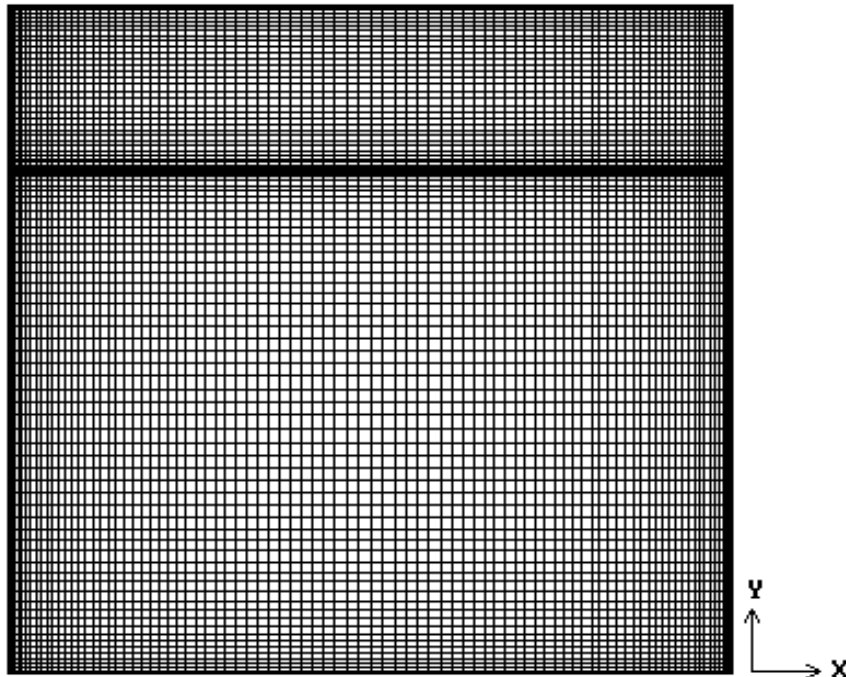


Figure 2. Computational cell structure and distribution for the top vented cases.

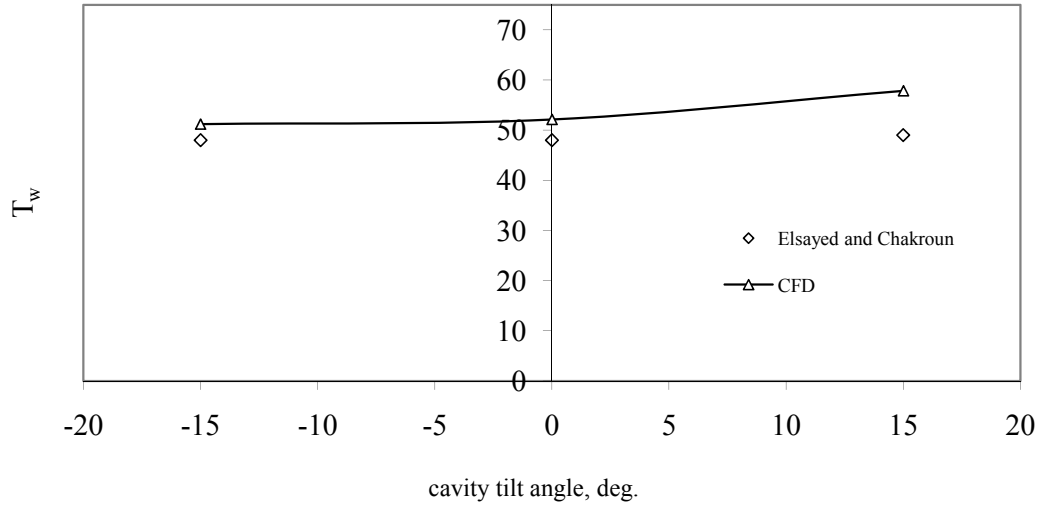


Figure 3. Comparison of present CFD results with experimental measurements by Elsayed and Chakroun (1999) for different cavity tilt angles.

ambient temperature. During calculations, the ambient temperature has been selected constant and equal to $T_{\infty}=22^{\circ}\text{C}$.

Velocity, pressure and temperature in the continuity, momentum and energy equations have been solved using boundary conditions given below:

Opening DE:

$$T_{\infty}=22^{\circ}\text{C}, P=P_{\infty}=0;$$

$$\frac{\partial u}{\partial x} = \frac{\partial v}{\partial x} = 0 \quad (5)$$

Wall boundary conditions:

The velocities are zero on AB, BC, CD and EA surfaces (no slip condition)

$$u = v = 0 \quad (6)$$

Constant heat flux on AB surface:

$$-k \left. \frac{\partial T}{\partial x} \right|_{AB} = q'' \quad (7)$$

Except for the surface subjected to a constant heat flux, all other surfaces have been assumed to be perfectly insulated,

$$\left. \frac{\partial T}{\partial y} \right|_{BC} = 0, \quad \left. \frac{\partial T}{\partial x} \right|_{CD} = 0, \quad \left. \frac{\partial T}{\partial y} \right|_{EA} = 0 \quad (8)$$

Dimensionless numbers affecting the heat transfer are given below:

Grashof number:

$$Gr_H = \frac{g\beta q'' H^4}{k\nu^2} \quad (9)$$

Rayleigh number:

$$Ra_H = Gr_H Pr \quad (10)$$

where the Pr number was assumed constant at 0.708

Nusselt number:

$$Nu = \frac{h_{avg} H}{k} \quad (11)$$

where h_{avg} is the average heat transfer coefficient obtained from the present numerical study and is defined by the relation:

$$h_{avg} = \frac{q''}{T_w - T_{\infty}} \quad (12)$$

SOLUTION ALGORITHM

The numerical model is based on a control volume-finite difference formulation. The above equations are integrated over each control volume to obtain a set of discretized linear algebraic equations of the form:

$$a_p \phi_p = \sum a_{nb} \phi_{nb} + s \quad (13)$$

Equations in the format given above are called finite volume equations. Finite volume equations describe processes affecting the value of ϕ , in cell P, in relation to its neighbor cells, together with the source terms. These equations were solved by the widely used commercial CFD package PHOENICS (Rosten and Spalding, 1987) employing the SIMPLEST algorithm

(Spalding, 1994) for the pressure correction process along with the solution procedure for the hydrodynamic equations. The package uses a staggered grid arrangement. Implicit temporal differencing is employed, and for the discretization of convective-diffusive transport, the hybrid scheme is the default scheme within the code (Patankar, 1980). This scheme combines the stability of the upwind-scheme with the approximation accuracy of the central-difference-scheme. In the hybrid-scheme, diffusion is cut off when the cell Peclet number ($Pe=RePr$, i.e. the ratio of heat convection to heat conduction) equals 2.0. In other words, the convective transport is assumed to dominate diffusive transport, and the hybrid-scheme reduces to the upwind formulation, with diffusion terms being neglected. The central-difference-scheme leads to second-order truncation error in the approximations, whereas the upwind-scheme gives only first order accuracy. The discretized equations are solved by the TDMA (Tri-Diagonal-Matrix-Algorithm).

RESULTS AND DISCUSSION

This numerical analysis was performed to study the effect of aperture geometry of a tilted, partially open cavity on the rate of heat transfer between the cavity and the surrounding air. The numerical analysis was conducted under different heat fluxes ranging from 0 W/m^2 to 480 W/m^2 with increments of 10 W/m^2 , different opening ratios of 0.25, 0.50 and 0.75, different tilt angles of -10° , 0° and 10° and different cavity aspect ratios of 1, 0.75 and 0.50, for top and center opening positions. The average Nusselt number of the heated wall was found to be dependent on the tilt angle of the cavity and the dimension and geometry of the aperture of the cavity.

The influence of the heat flux on the average Nusselt number (Nu), for different opening ratios (OR) is demonstrated in Fig. 4 for different tilt angles (θ) of the cavity. As can be seen from Figs. 4(a), (b) and (c), average Nusselt number increases with the heat flux. When the figures are examined carefully, rate of average Nusselt number increases rapidly at low heat fluxes and then reaches almost constant values for all opening ratios. Figures also show that the average Nusselt number decreases with decrease of the opening ratio. When the opening ratio decreases, air circulation inside the cavity slows down, hence resulting in a decrease in the rate of heat transfer to the surroundings. For opening ratios of 0.75 and 0.50, the values of average Nusselt number are bigger than that of OR=0.25. Better heat transfer is obtained for higher values of the opening ratios. With the increase of the tilt angle and decrease of the opening ratio, Nusselt number decreases. Especially the decrement at the tilt angle of 10° and OR=0.25 is more than at the other values of angles and opening ratios.

Fig. 5 presents variations of the average Nusselt number with Rayleigh number, for different opening ratios.

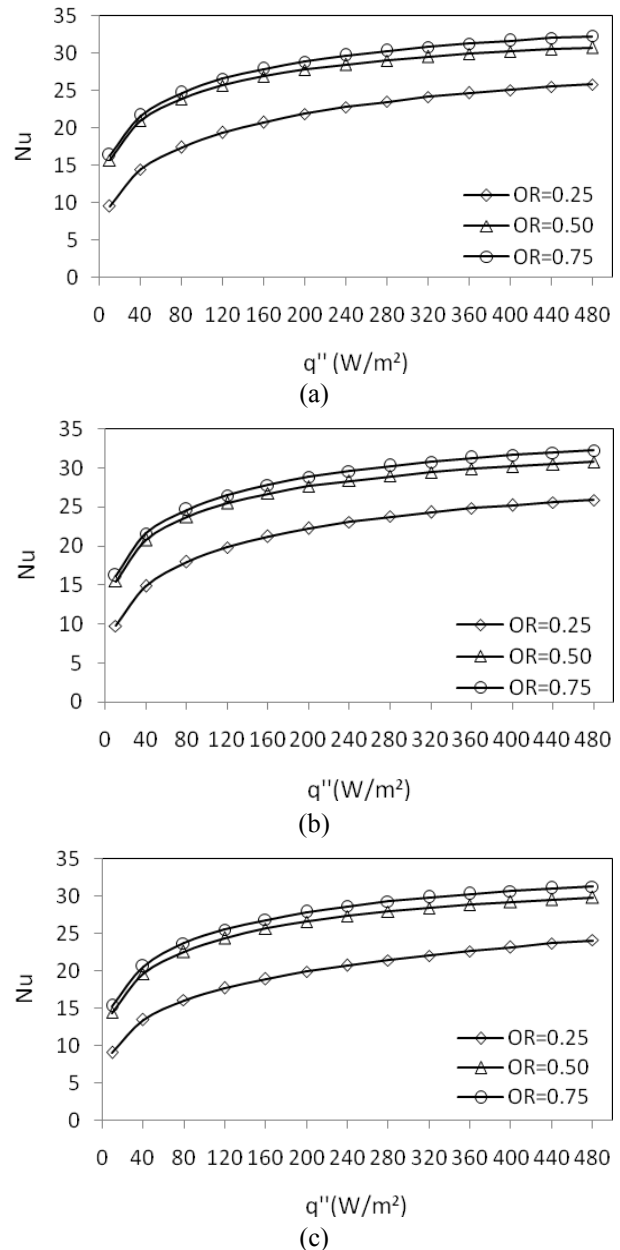
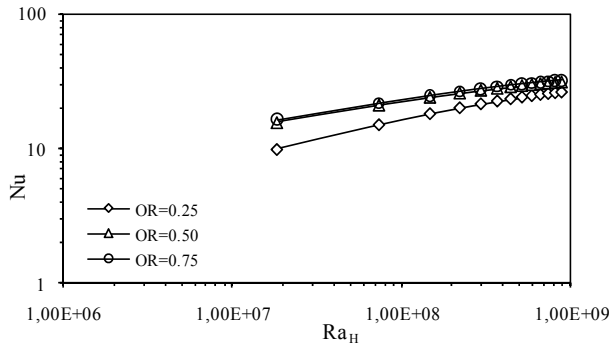
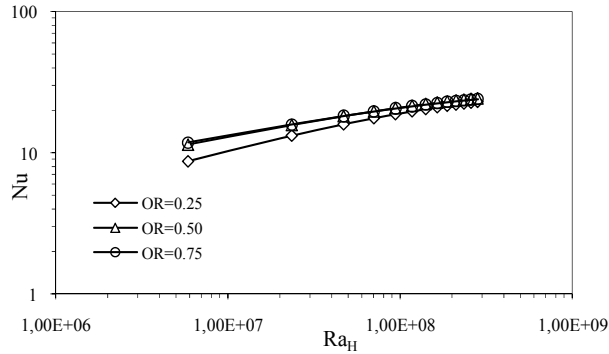


Figure 4. Effect of OR on the Nu number for various heat flux with $\theta = -10^\circ$, 0° , and 10° , respectively (AR=1, top

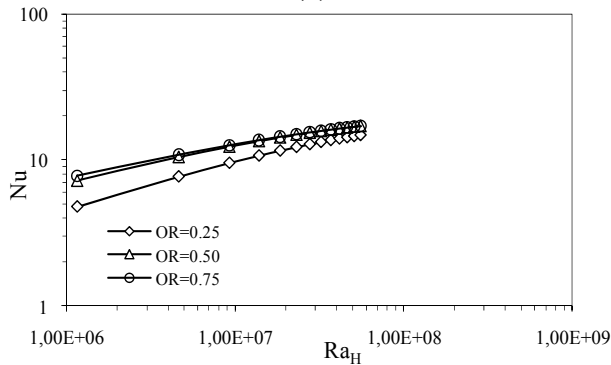
Results are for the top vented position at $\theta=0^\circ$. Data for opening ratios of 0.25, 0.50, and 0.75 are presented. As shown in the Figs. 5 (a), (b), (c) average Nusselt number increases continuously with the increase of the Rayleigh number. For the same Rayleigh number, the average Nusselt number increases with increase of opening ratio. While the Rayleigh numbers reach their maximum values (in the range of solutions obtained in the present study), lines of the average Nusselt numbers approach each other for all opening ratios. Furthermore, as Rayleigh number increases, convection increases and the heat transfer is dominated by convection for all opening ratios. Moreover, the average Nusselt number and Rayleigh number approach each other for the aspect ratio of 0.5 and 0.75 respectively. On the other hand, the variation of average Nusselt number according to Rayleigh number for opening ratio of 0.25 is lower than



(a)



(b)

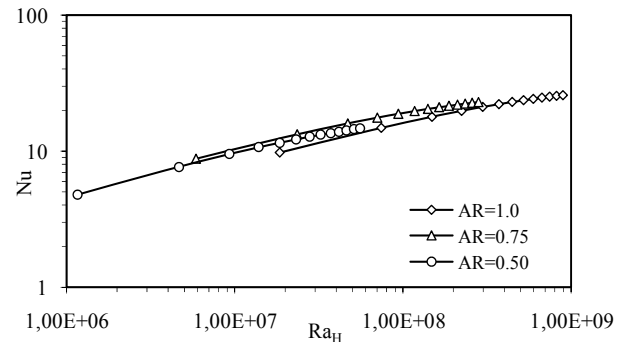


(c)

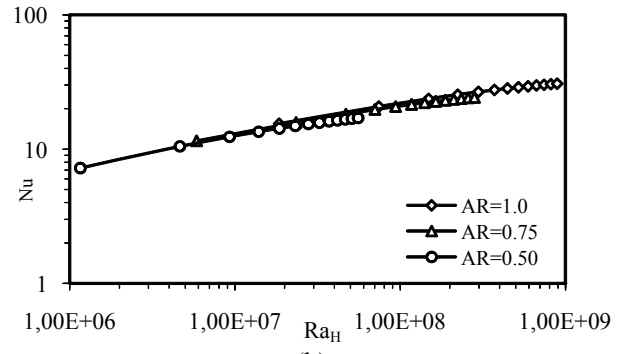
Figure 5. Effect of OR on the Nu number for various Ra_H with $AR=1.0, 0.75$, and 0.5 , respectively ($\theta=0^\circ$, top vented).

those of the other opening ratios. Fig. 6 shows the effect of aspect ratio on average Nusselt number, for various Rayleigh numbers, with different opening ratios, for tilt angle of 0° and the top vented case. For the $OR=0.25$, the maximum value of average Nusselt number for $AR=0.50$ is greater than that of the initial value of $AR=1$, and lower than maximum value of Nusselt number for $AR=0.75$, as shown in Fig. 6 (a). For $OR=0.50$, the curves of the average Nusselt number almost overlap for all the aspect ratios. Because of dominated convective flow, minimum value of average Nusselt number for $AR=1$ is bigger than those of $AR=0.75$ and 0.50 as shown in Fig. 6 (b). In all the figures, the heat transfer increases with increase of Rayleigh number for all aspect ratios and opening ratios.

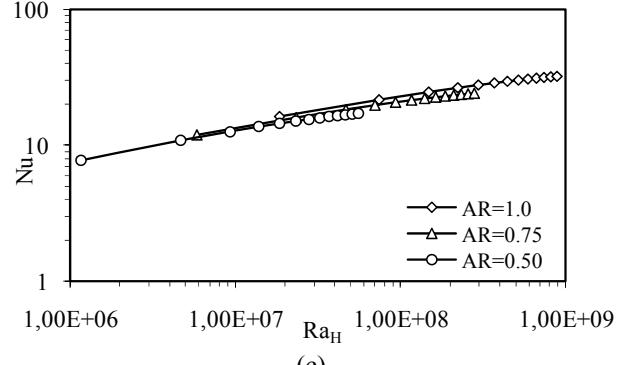
Fig. 7 shows the effect of opening ratio on average Nusselt number for various Rayleigh numbers, with different tilt angles, for $AR=1$ and center vented case.



(a)



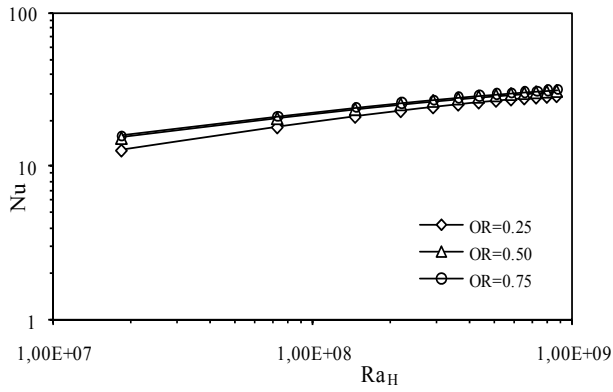
(b)



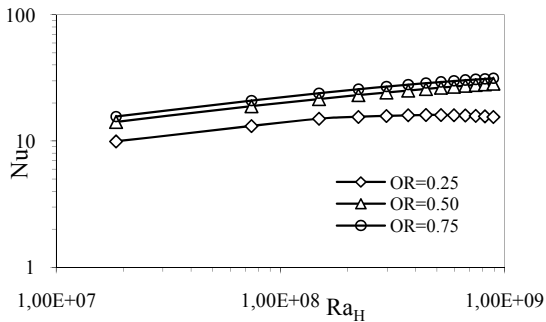
(c)

Figure 6. Effect of AR on the Nu number for various Ra_H with $OR=0.25, 0.50$, and 0.75 , respectively ($\theta=0^\circ$, top

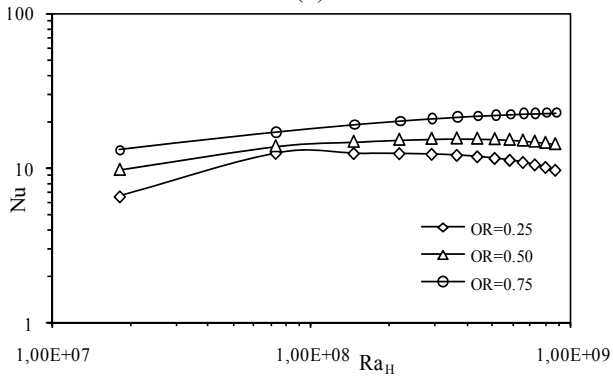
Average Nusselt number increases with Rayleigh number for all opening ratios at tilt angle -10° , and the values of Nusselt number are close to each other as seen in Fig.7 (a). At high Rayleigh numbers, the effects of buoyancy-driven flow on average Nusselt number becomes more important. However, average Nusselt number increases up to a certain Rayleigh number of about 4.46×10^8 , and then slightly decreases at tilt angle 0° and opening ratio of 0.25 , as shown in Fig 7(b). This decrement leads to the increase of the temperature and so the lower heat transfer rate in the cavity. In Fig. 7 (c), especially for the opening ratio of 0.25 , the average Nusselt number increases linearly for relatively high values of Rayleigh number but, as Rayleigh number increases to about 10^8 , the variation of Nusselt number deviates from its linear variation for the tilt angle of 10° . As can be seen, at high Rayleigh numbers, convective heat transfer rate increases, but it also decreases with a positive tilt angle and decrease of opening ratios.



(a)



(b)

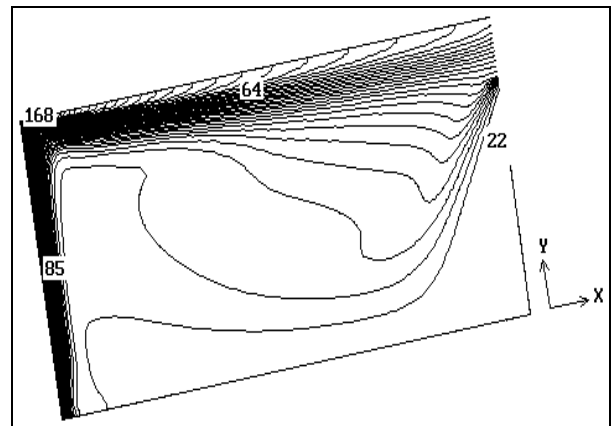


(c)

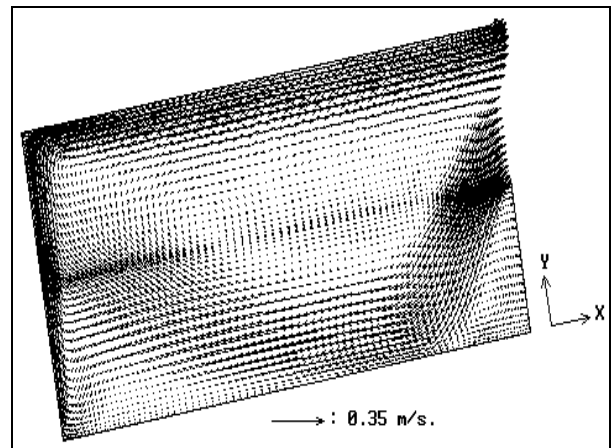
Figure 7. Effect of OR on the Nu number for various Ra_H with $\theta = -10^\circ, 0^\circ,$ and 10° , respectively ($AR=1$, center

For all investigated cases velocity vector distributions, temperature contours were drawn. It is impossible to show all these results. Therefore, as an example, the temperature contours and velocity vectors inside the cavity for $q''=480 \text{ W/m}^2$, $\theta = -10^\circ$, $AR=0.50$ and $OR=0.50$ are given in Fig. 8. As illustrated by Fig. 8(a), the cold fluid entrained through the larger section of the opening moves across the cavity following the lower bounding wall, rises along the hot wall, moves across the upper part following the top bounding wall and discharges at the opening. The temperature contours show formation of boundary layer heat transfer along the heated wall. The temperature of the inside air increases towards the top left corner of the partial enclosure. For $q''= 480 \text{ W/m}^2$ the intensity of the convection is rather strong, which implies that the convection heat transfer begins dominating the thermal flow field inside the cavity. It is seen that as heat flux

increases, flow becomes fully convection dominated, the cold fluid is entrained right to the hot wall where high temperature gradients are created, and the discharging fluid from the upper part of the cavity occupies smaller and smaller sections of the opening, being like a jet at high heat fluxes. As a consequence of increasing convective motion with increasing heat flux, the temperature gradient near the heated wall becomes more affective and colder fluid tends to occupy a lower part of the cavity. Some difficulty is observed, in other cases, in entering the fresh air, when the inside air temperature rises at high heat flux conditions. Under these conditions, fresh air entering the cavity is heated very quickly to relatively high temperatures, hindering the fresh air intake during exhaust. Moreover, heat transfer decreases because air circulation activity slows down. Better heat transfer characteristics were obtained at lower heat fluxes. The velocity vectors are depicted in Fig. 8 (b). As shown in the figure, ascending warmer air which is lifted along the hot wall moves upward, and it flows parallel to the adiabatic top wall. While the hot air exits at the top side of the opening, cold ambient air enters the cavity easily at the bottom side of the opening.



(a)



(b)

Figure 8. Temperature contours and velocity vector plots, respectively, for $q''=480 \text{ W/m}^2$, $\theta = -10^\circ$, $AR=0.50$, $OR=0.50$.

Figures 9 to 11 show a compilation of the effects of various parameters to fluid flow inside the partially open cavity. Fig. 9(a), Fig. 10(a) and Fig. 11(a) show that the rate of fresh air entering the cavity increases with the increase of the opening ratio, at tilt angle -10° . Due to the fact that the buoyancy driven flow is more effective in the cavity, good air circulation is observed. Therefore, larger heat transfer rates were obtained. Fig. 9(b), Fig. 10(b) and Fig. 11(b) show fluid flow characteristics inside the cavity for different opening ratio at the tilt angle of 0° . As can be seen from the figures, again the fresh air rate increases with increase

in the opening ratio. With increase in the aspect ratio, after touching the heated surface, the warm air leaves the cavity via an increasing distance from the hot surface. Better heat transfer results are obtained for larger aspect ratios. Fig. 9(c), Fig. 10(c) and Fig. 11(c) show that the entering fresh air moves upwards at the heated surfaces, detaching itself at about half height as a result of gravity effects, at a tilt angle of 10° , for different opening ratios. The detaching flow for these cases hinders a full circulation of air inside the cavity, and as a result reduces the heat transfer rate. For all the cases, small changes of fluid flow characteristics were

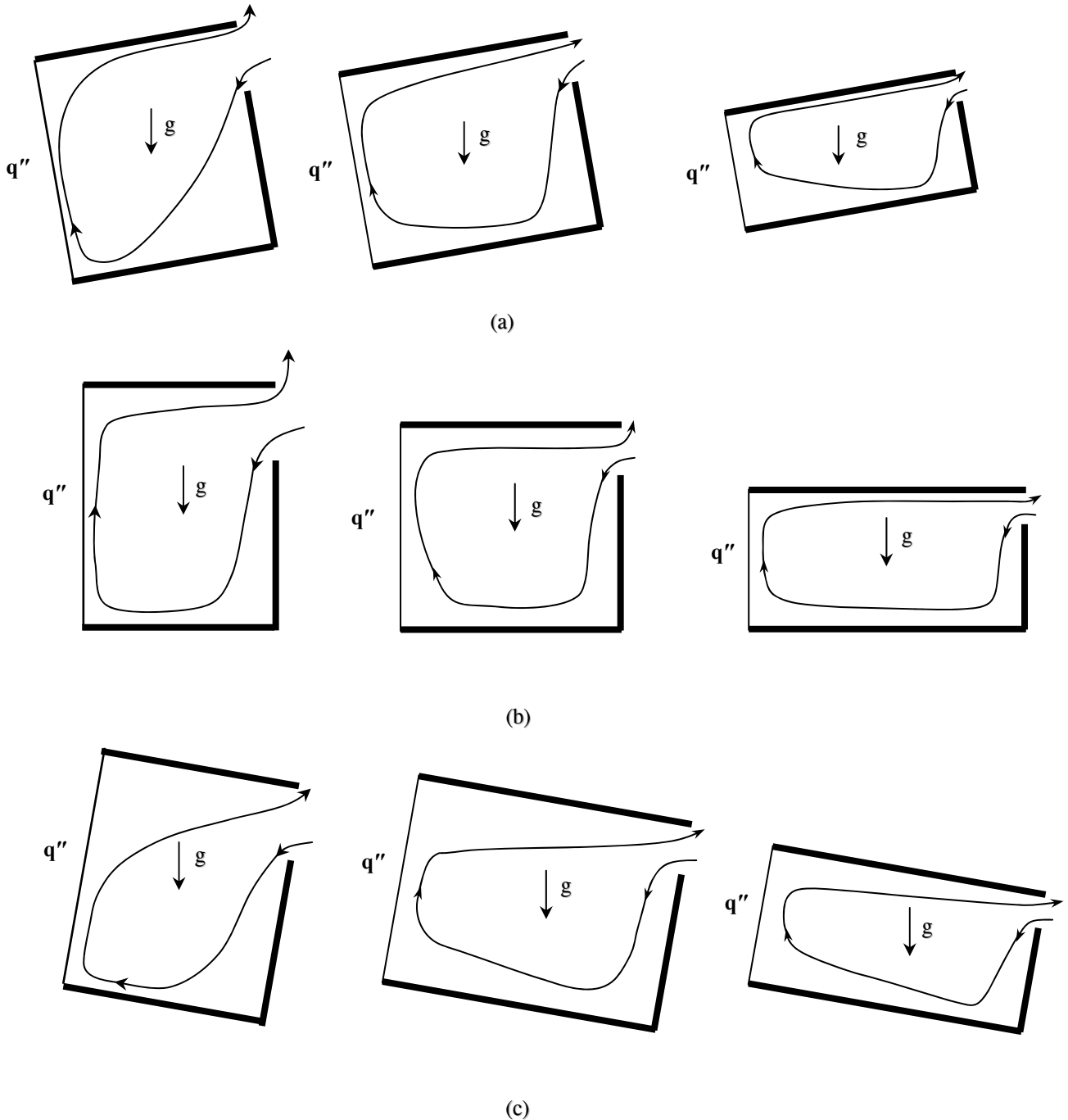


Figure 9. Effect of various parameters on heat transfer and fluid flow for OR=0.25, top vented.
a) $\theta = -10^\circ$: AR=1.0, 0.75, 0.50
b) $\theta = 0^\circ$: AR=1.0, 0.75, 0.50
c) $\theta = 10^\circ$: AR=1.0, 0.75, 0.50

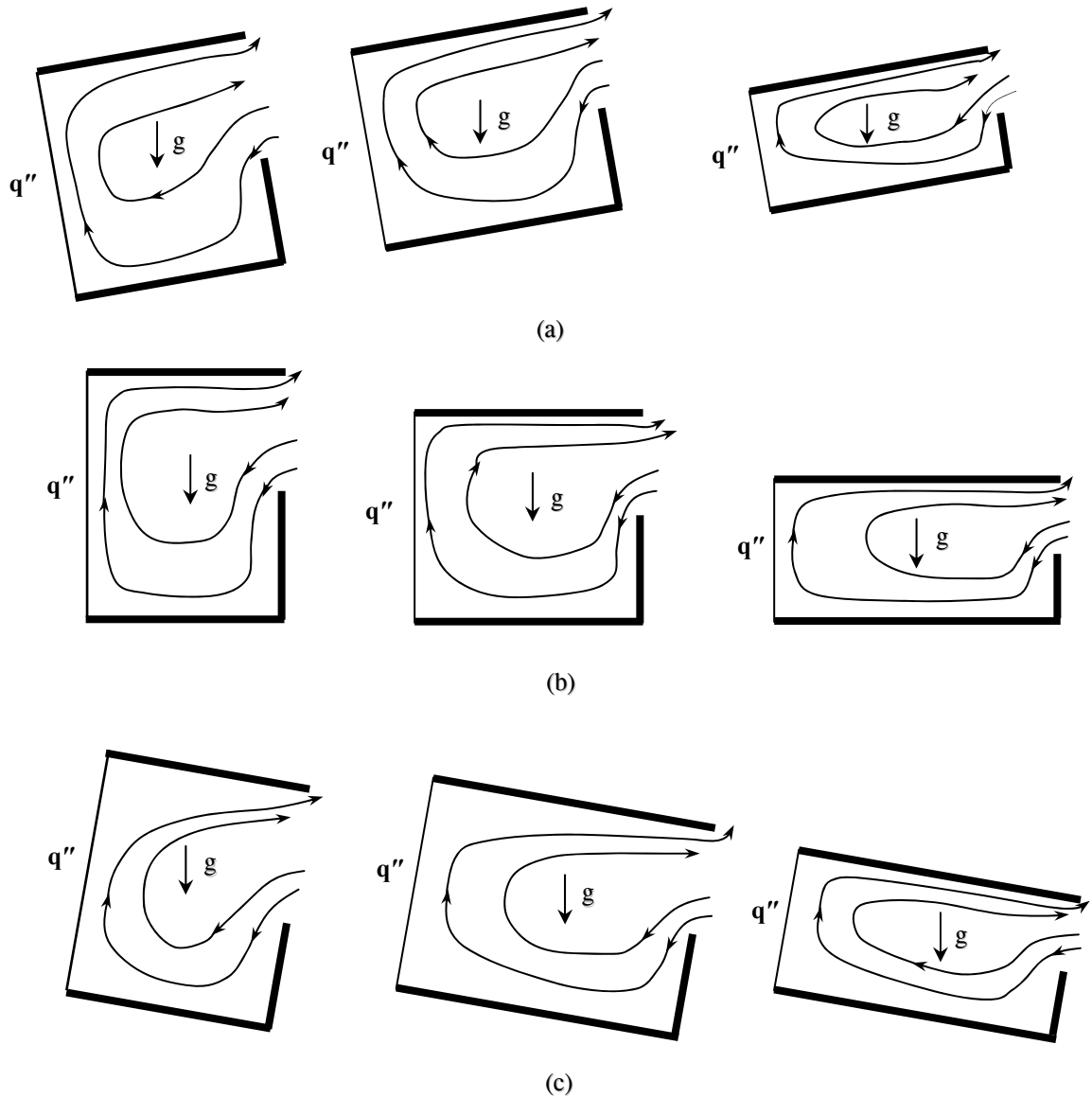


Figure 10. Effect of various parameters on heat transfer and fluid flow for OR=0.50, top vented.

- a) $\theta = -10^\circ$: AR=1.0, 0.75, 0.50
 b) $\theta = 0^\circ$: AR=1.0, 0.75, 0.50
 c) $\theta = 10^\circ$: AR=1.0, 0.75, 0.50

observed between the negative inclination (-10°) and the vertical orientation (0°). Significant flow changes were obtained for the positive inclination (10°).

The effect of various parameters on heat transfer and fluid flow for different opening ratios for the center vented position is presented in Fig. 12. Although average surface temperature increases, average Nusselt number decreases for aspect ratio of 1. Because of increasing tilt angle to the negative direction and increasing the opening ratio, it is observed that the average surface temperature decreases conversely with the increase of average Nusselt number. The entering fresh air shows good circulation because of the buoyancy driven flow inside the cavity for tilt angle of -10° , and better heat transfer is obtained than that of the other tilt angles.

CONCLUSIONS

In this study, steady-state laminar natural convection heat transfer from rectangular, tilted, partially open cavities has been investigated numerically. The cavity was formed by an adiabatic wall, a heated wall facing the partial opening and the whole cavity was tilted. Different geometrical parameters were considered, such as aspect ratio (AR=1, 0.75, 0.50), opening ratio (OR=0.25, 0.50, 0.75), different tilt angles ($\theta=-10^\circ, 0^\circ, 10^\circ$), for top and center opening positions. One side of the cavity was subjected to different heat fluxes. Equations of mass, momentum and energy have been solved employing computational fluid dynamics techniques.

Overall, the obtained results show that the heat transfer is affected by all parameters, as a result of the changes in the fluid flow characteristics of air inside the cavity,

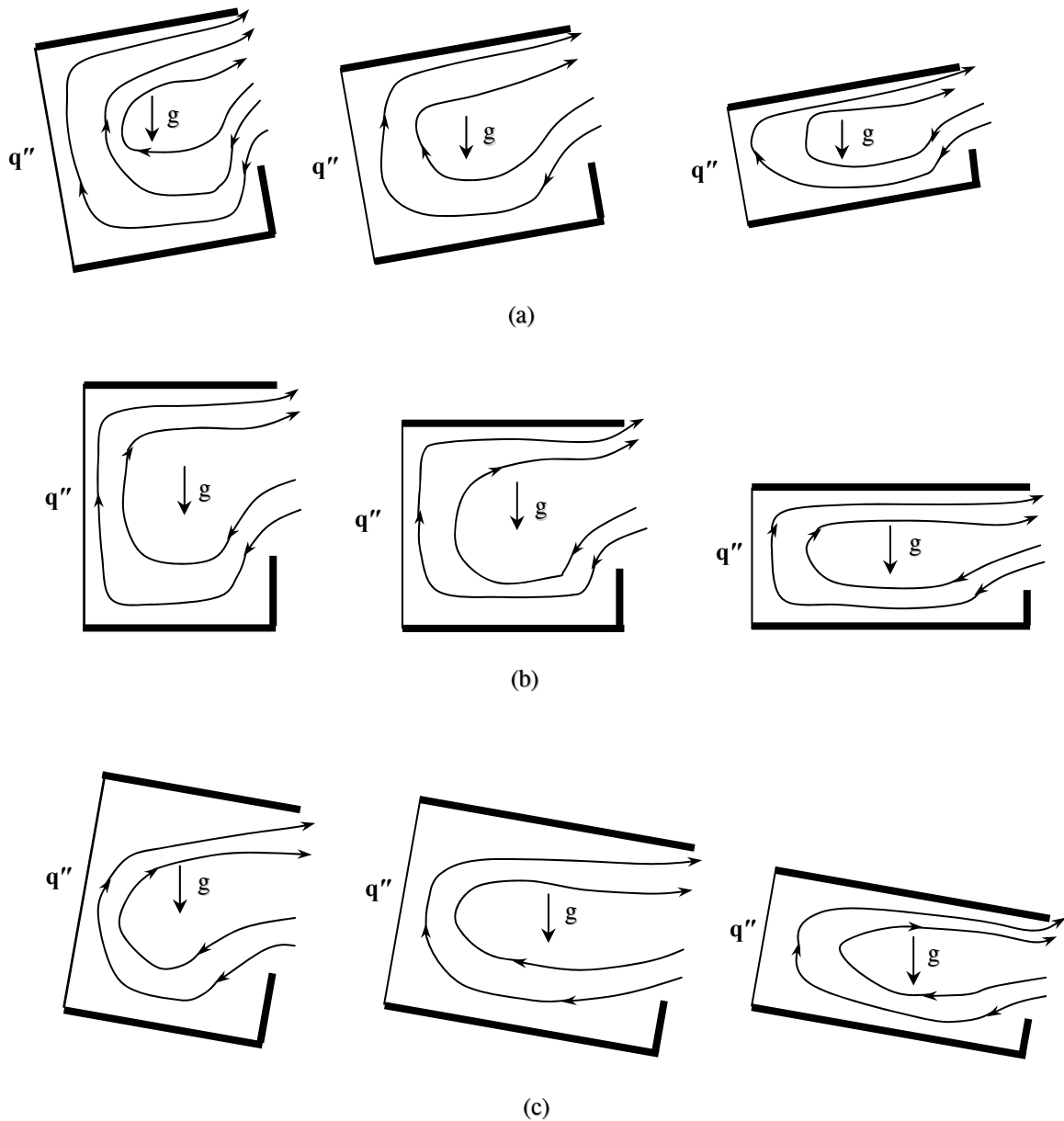


Figure 11. Effect of various parameters on heat transfer and fluid flow for OR=0.75, top vented.

a) $\theta = -10^\circ$: AR=1.0, 0.75, 0.50

b) $\theta = 0^\circ$: AR=1.0, 0.75, 0.50

c) $\theta = 10^\circ$: AR=1.0, 0.75, 0.50

due to changes of these parameters. For the top vented case, the average Nusselt number increases with increase of opening ratio and decrease of tilt angle for all aspect ratios. At tilt angle of -10° , with the increase of the opening ratio, buoyancy driven flow is more effective inside the cavity, hence, good air circulation is observed. For the center vented case, for AR=1, Nusselt number decreases with the increase of the average surface temperature. Increase of the opening ratio and the tilt angle to the negative direction increases the heat transfer rate. As a consequence, best heat transfer was observed for an aspect ratio of 1, opening ratio of 0.75 and tilt angle of -10° .

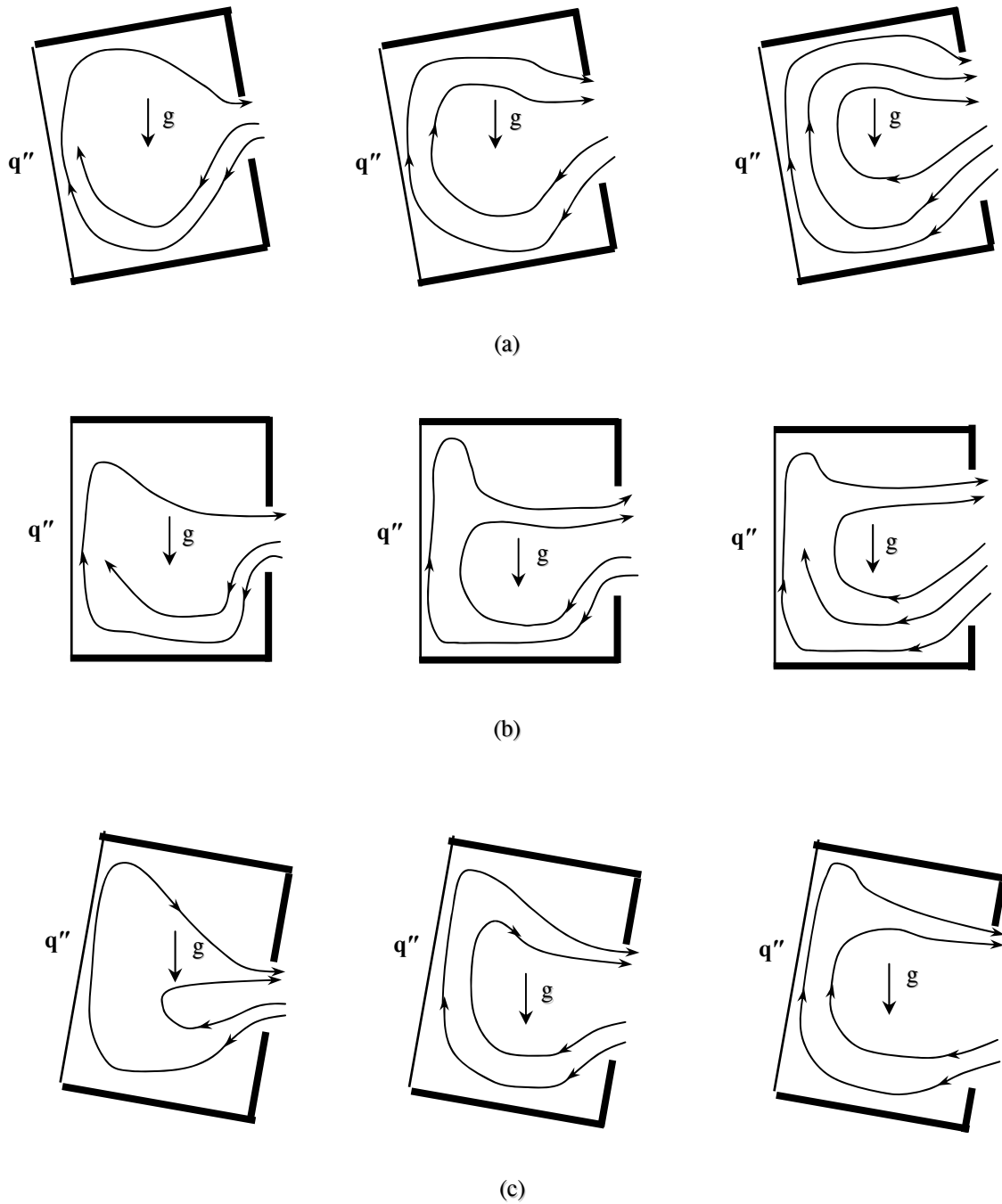


Figure 12. Effect of various parameters on heat transfer and fluid flow for AR=1.0, center vented.
a) $\theta = -10^\circ$: OR=0.25, 0.50, 0.75
b) $\theta = 0^\circ$: OR=0.25, 0.50, 0.75
c) $\theta = 10^\circ$: OR=0.25, 0.50, 0.75

REFERENCES

Arcidiacono S., Di Piazza I., Ciofalo M., Low-Prandtl number natural convection in volumetrically heated rectangular enclosures II. Square cavity, AR=1, *Int. J. Heat Mass Transfer* 44, 537-550, 2001.

Aydin O., Ünal A., Ayhan T., Natural convection in rectangular enclosures heated from one side and cooled from the ceiling, *Int. J. Heat Mass Transfer* 42, 2345-2355, 1999.

Basak T., Roy S., Balakrishnan A.R., Effects of thermal boundary conditions on natural convection flows within a square cavity, *Int. J. Heat Mass Transfer* 49, 4525-4535, 2006.

Bilgen E., Oztop H., Natural convection heat transfer in partially open inclined squire cavities, *Int. J. Heat Mass Transfer* 48, 1470-1479, 2005.

Chang T. S., Tsay Y. L., Natural convection heat transfer in an enclosure with a heated backward step, *Int. J. Heat Mass Transfer* 44, 3963-3971, 2001.

- Costa V. A. F., Laminar natural convection in differentially heated rectangular enclosures with vertical diffusive walls, *Int. J. Heat Mass Transfer* 45, 4217-4225, 2002.
- Di Piazza I., Ciofalo M., Low-Prandtl number natural convection in volumetrically heated rectangular enclosures I. Slender cavity, AR=4, *Int. J. Heat Mass Transfer* 43, 3027-3051, 2000.
- Elsayed M., Chakroun M. W., Effect of aperture geometry on heat transfer in tilted partially open cavities, *Journal Heat Transfer* 121, 819-827, 1999.
- Kasayapanand N., Numerical modeling of natural convection in partially open cavities under electric field, *Int. Comm. Heat Mass Transfer* 34, 630-643, 2007.
- Leong K. C., Tan F. L., Experimental study of freezing in a rectangular enclosure, *Journal of Materials Processing Technology* 70, 129-136, 1997.
- Nithyadevi N., Kandaswamy P., Lee J., Natural convection in a rectangular cavity with partially active side walls, *Int. J. Heat Mass Transfer* 50, 4688-4697, 2007.
- Patankar S.V., *Numerical Heat Transfer and Fluid Flow*, Hemisphere, New York, 1980.
- Polat O., Bilgen E., Laminar natural convection in inclined open shallow cavities, *Int. J. Therm. Sci.* 41, 360-368, 2002.
- Poujol F. T., Natural convection of a high Prandtl number fluid in a cavity, *Int. Comm. Heat Mass Transfer* 27, 109-118, 2000.
- Rosten H., Spalding D.B., *The PHOENICS Beginners Guide*, CHAM 1. Ltd., London, 1987.
- Salat J., Xin S., Joubert P., Sergent A., Penot F., Le Quere P., Experimental and numerical investigation of turbulent natural convection in a large air-filled cavity, *Int. J. Heat Fluid Flow* 25, 824-832, 2004.
- Spalding D.B., *The PHOENICS Encyclopedia*, CHAM Ltd., London, 1994.